XY-Theta Positioning Table with Parallel Kinematics and Unlimited Theta Rotation

Ilian A. Bonev [1], Alexander Yu [2], Paul Zsombor-Murray[2]
[1]Department of Automated Manufacturing Engineering, École de Technologie Supérieure, Montreal, QC, Canada
ilian.bonev@etsmtl.ca
[2]Department of Mechanical Engineering, McGill University, Montreal, QC, Canada

***Abstract*—Parallel robots are increasingly being used in industry for positioning and alignment. They have the advantage of being rigid, quick, and accurate. However, most parallel robots have very limited rotational capabilities and in cases where unlimited rotation is necessary, the only option used to be adding a rotary table. There however exists one overlooked XY-Theta parallel robot design that can reach any point within a circular workspace at any orientation. This unique design consists of three pivots moving independently along a common circular path. These pivots are connected individually to three linear guides attached to a mobile platform in a symmetric "Y" shape. By studying the kinematics of this parallel robot, this paper shows that not only is the dextrous workspace large but the kinematic accuracy is high and uniform.**

I. Introduction

Workspace capabilities were never a strong point for any parallel robot structure [1]. Particularly, orientations achieved by these robots are typically very limited and depend on the position of the mobile platform. To increase the rotation capabilities of some parallel robots, additional motors are usually added in series. This however, increases the inertia of the mobile part, thus reducing the speed of the robot.

Probably the only 6-degree-of-freedom (DOF) fully-parallel robot that has unlimited rotational capabilities about an axis is the Rotopod [2], commercialized by the Parallel Robotic Systems Corporation (Fig. 1). In this parallel robot, six legs of fixed length connect a mobile platform to a base, through spherical joints. The centers of the base spherical joints move independently along a common circular path under the action of six motors.

There exists a very similar planar parallel robot, which is however still unknown to the public [3]. This parallel robot has a rare architecture (joint sequence) that, although well known and previously studied in the literature [4], has never been given any particular interest. It is a peculiar design that features a unique circular path, on which all intermediate revolute joints move. These joints slide along three linear guides attached to the mobile platform in a symmetric "Y" shape. The resulting mechanism has a singularity-free circular workspace (under the natural assumption that the linear guides have limited lengths) in which any orientation can be achieved. Furthermore, the dexterity of this robot is fairly high and uniform.

Fig. 1. The Rotopod R-series hexapod (courtesy of PRSCo).

This paper will analyze the kinematics of this unknown parallel robot in the following sections. It will be shown that the direct and the inverse kinematics for this robot are simple, that its singularities are outside the feasible workspace that is inside the circular track. Finally, the local dexterity analysis of this robot will reveal that the robot is fairly accurate within its range of motion.

II. Brief Description of the Parallel Robot

In this paper, the term *linear bearing* will be used to refer to the linear segment on the mobile platform along which a pivot, denoted by O_i (i = 1, 2, 3), may translate (Fig. 2). Naturally, it is assumed that these linear bearings (or linear guides) have finite lengths and form a symmetric "Y" shape. The pivots within those linear bearings travel along a circular path, which allows the robot to rotate without limits about the center of the circular path, when all motors move at the same rate.

A base reference frame Oxy is fixed at the center of the circular path, and a mobile reference frame $Cx'y'$ is fixed at the center of the mobile platform in such a way that the y' axis coincides with linear bearing 2.

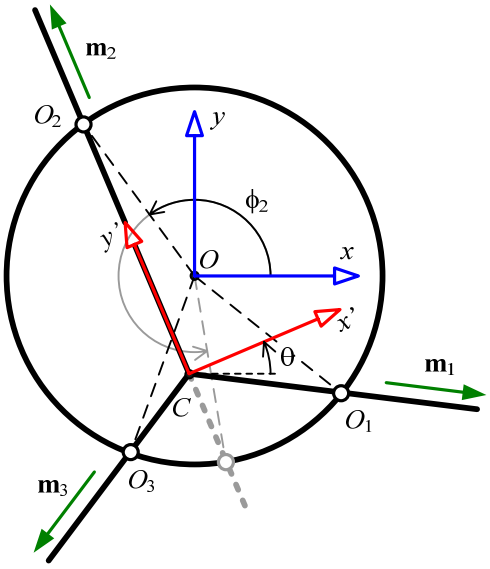

Fig. 2. Schematic of the parallel robot under study.

Let the angle between the base x axis and the mobile x' axis be denoted by θ (the *orientation* of the mobile platform) and the coordinates of point C (the intersection of the three linear bearings) with respect to the base frame (the *position* of the mobile platform) be denoted by x and y. The position (x, y) and orientation (θ) of the mobile platform will be referred to as the *pose* of the mobile platform. On the other hand, the location of points O_i on the circular path is defined by the angle ϕ_i, which is the angle between the base x axis and the vector OO_i. The three angles ϕ_i will be referred to as the *input variables*.

Finally, for simplicity, it is assumed that the radius of the circular path is of unit length.

III. Inverse Kinematics

The inverse kinematic problem is to find the input variables that correspond to a given pose of the mobile platform. Geometrically, solving the inverse kinematic problem of this mechanism consists of finding the intersection points of lines CO_i with the circular path. Thus, for a given pose of the mobile platform, this mechanism allows two possible solutions for each input variable (Fig. 2), assuming that point C is inside the circular path. However, for only one of each of the two solutions, the corresponding point O_i is inside the linear bearings. Thus, there is only one practically realisable (i.e., feasible) solution for the input variable ϕ_i.

Let us denote then by $\mathbf{m}_i$ the unit vector along each linear bearing, directed outwards as shown in Fig. 2. By definition, we have:

$$\mathbf{m}_i = \begin{bmatrix} \cos\theta_i \\ \sin\theta_i \end{bmatrix}, \tag{1}$$

where

$$\theta_i = \theta - \frac{\pi}{6} + \frac{2\pi}{3}(i-1). \tag{2}$$

The following vector equation can now be written:

$$\overrightarrow{CO_i} = \overrightarrow{OO_i} - \overrightarrow{OC}. \tag{3}$$

It yields two algebraic equations:

$$\rho_i \cos\theta_i = \cos\phi_i - x, \tag{4}$$

$$\rho_i \sin\theta_i = \sin\phi_i - y, \tag{5}$$

where ρ_i is the distance (positive or negative) from C to O_i along $\mathbf{m}_i$. Combining the above two equations to eliminate ρ_i and rearranging leads to the following simple equation that defines the inverse kinematic problem:

$$\sin(\phi_i - \theta_i) = y\cos\theta_i - x\sin\theta_i. \tag{6}$$

In order to have a solution for the above equation, its right-hand side should be between –1 and +1. It can be easily shown that this right-hand side is actually the directed distance from O to linear bearing i, and this distance should be less than 1 in order to have a solution. Thus, assuming that point C is inside the circular path, the two solutions for leg i are:

$$\phi_i = \theta_i + \arcsin(y\cos\theta_i - x\sin\theta_i) \tag{7}$$

and

$$\phi_i = \pi + \theta_i - \arcsin(y\cos\theta_i - x\sin\theta_i). \tag{8}$$

It can be shown that only the first solution is feasible, i.e., point O_i is inside the linear bearing.

IV. Direct Kinematics

The direct kinematic problem is to find the pose of the mobile platform that corresponds to a given set of input variables. For a given set of input variables (i.e., given points O_i), this mechanism allows theoretically two poses for the mobile platform [6]. Both poses have the same position but a 180º difference in the orientation. However, only one of these poses is practically realisable (i.e., points O_i are inside the linear bearings). Furthermore, it can be easily shown, that if any of the angles of triangle $O_1O_2O_3$ is greater than 120º, then the center C would have to be outside the circular path, which means that both poses will not be practically realisable.

Assuming that none of the angles of the triangle $O_1O_2O_3$ is greater than 120º, the corresponding practically realisable pose can be easily obtained through the following geometric construction, based on the notion of *first Fermat point*.

In any triangle $O_1O_2O_3$ in which none of the angles is greater than 120º (Fig. 3), if equilateral triangles are constructed outside triangle $O_1O_2O_3$ and their extreme vertices (points P_i) are connected with the opposite vertices of triangle $O_1O_2O_3$, the resulting lines (P_iO_i) will intersect at a single point. This point, F, is called first Fermat point (also known as Torricelli point, or first isogonic center) and has the property that all inscribed angles are equal, i.e., $\angle O_1FO_3 = \angle O_3FO_2 = \angle O_2FO_1 = 120º$. (This point also has the interesting property that it minimizes the sum of the distances to the vertices of the triangle $O_1O_2O_3$.) Therefore, this first Fermat point is actually the center point C.

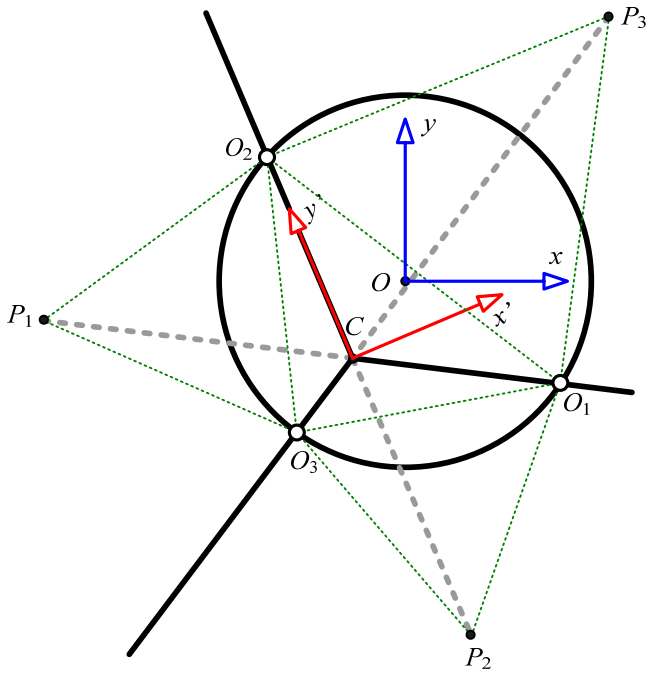

Fig. 3. Solving the direct kinematics of the parallel robot under study.

To find the coordinates of point C and the orientation, θ, of the mobile platform, the following simple calculations will be performed. Let $\mathbf{p}_i$ denotes the vector connecting point O to point P_i. Therefore, it can be easily shown that vector $\mathbf{p}_i$ can be written as:

$$\mathbf{p}_i \equiv \begin{bmatrix} x_{p_i} \\ y_{p_i} \end{bmatrix} = \frac{1}{2}(\mathbf{o}_j + \mathbf{o}_k) + \frac{\sqrt{3}}{2}\mathbf{E}(\mathbf{o}_j - \mathbf{o}_k), \tag{9}$$

where

$$\mathbf{E} = \begin{bmatrix} -1 & 0 \\ 0 & 1 \end{bmatrix}, \tag{10}$$

and (i, j, k) = (1, 2, 3) or (2, 3, 1) or (3, 1, 2). Now, taking lines O_1P_1 and O_2P_2, for example, their intersection point is C and has the following coordinates:

$$x = \frac{\left(x_{O_1}y_{P_1} - x_{P_1}y_{O_1}\right)\left(x_{O_2} - x_{P_2}\right) - \left(x_{O_2}y_{P_2} - x_{P_2}y_{O_2}\right)\left(x_{O_1} - x_{P_1}\right)}{\left(x_{O_1} - x_{P_1}\right)\left(y_{O_2} - y_{P_2}\right) - \left(x_{O_2} - x_{P_2}\right)\left(y_{O_1} - y_{P_1}\right)}, \tag{11}$$

$$y = \frac{\left(x_{O_1}y_{P_1} - x_{P_1}y_{O_1}\right)\left(y_{O_2} - y_{P_2}\right) - \left(x_{O_2}y_{P_2} - x_{P_2}y_{O_2}\right)\left(y_{O_1} - y_{P_1}\right)}{\left(x_{O_1} - x_{P_1}\right)\left(y_{O_2} - y_{P_2}\right) - \left(x_{O_2} - x_{P_2}\right)\left(y_{O_1} - y_{P_1}\right)}. \tag{12}$$

Finally, the orientation of the mobile platform remains to be found. This can be done by measuring the angle between vector CO_2, and the base y axis:

$$\theta = \text{atan2}\left(y - y_{O_2}, x - x_{O_2}\right) - \frac{\pi}{2}. \tag{13}$$

V. Velocity Analysis

Next, the relationship between the rates of the input variables (i.e., the *input rates*) and the linear and angular velocity of the mobile platform at its center C (i.e., the *output rates*) need to be found. These will be necessary nor only for calculating the speed of displacements but also for evaluating the local dexterity of the parallel robot under study. This is done by differentiating (6) with respect to time, and after rearranging and writing in matrix form, the following is obtained:

$$\begin{bmatrix} -\sin\theta_i & \cos\theta_i & \rho_i \end{bmatrix} \begin{bmatrix} \dot{x} \\ \dot{y} \\ \dot{\theta} \end{bmatrix} = \cos(\phi_i - \theta_i)\dot{\phi}_i. \tag{14}$$

This equation can also be written in matrix form as:

$$\begin{bmatrix} \mathbf{E}\mathbf{m}_i & \rho_i \end{bmatrix} \dot{\mathbf{q}} = \mathbf{m}_i^T \mathbf{o}_i \dot{\phi}_i. \tag{15}$$

Finally, writing the above equation for all values of i and placing the resulting equations in matrix form, yields:

$$\mathbf{Z}\dot{\mathbf{q}} \equiv \begin{bmatrix} \mathbf{E}\mathbf{m}_1 & \rho_1 \\ \mathbf{E}\mathbf{m}_2 & \rho_2 \\ \mathbf{E}\mathbf{m}_3 & \rho_3 \end{bmatrix} \dot{\mathbf{q}} = \begin{bmatrix} \mathbf{m}_1^T\mathbf{o}_1 & 0 & 0 \\ 0 & \mathbf{m}_2^T\mathbf{o}_2 & 0 \\ 0 & 0 & \mathbf{m}_3^T\mathbf{o}_3 \end{bmatrix} \dot{\boldsymbol{\phi}} \equiv \boldsymbol{\Lambda}\dot{\boldsymbol{\phi}}. \tag{16}$$

Thus, the Jacobian matrix of this parallel robot is

$$\mathbf{J} = \boldsymbol{\Lambda}^{-1}\mathbf{Z}. \tag{17}$$

VI. Singularities

Singularities are special configurations at which the velocity equation (16) degenerates, i.e., one or both matrices $\mathbf{Z}$ and $\boldsymbol{\Lambda}$ become singular. We see that $\boldsymbol{\Lambda}$ is singular when a linear bearing is tangent to the circular path. This implies that the center C will be outside or on the circular path, which means that some ρ_i will be negative, which is an unfeasible configuration. Therefore, we may state that, as long as the pivots remain inside the linear bearings, there will be no such singularity.

The geometric interpretation of matrix $\mathbf{Z}$ is more difficult to see without some background in line geometry. The rows of this matrix are in fact the line coordinates of the lines normal to the linear bearings and passing through the pivots O_i, expressed in the mobile frame. This means that matrix $\mathbf{Z}$ is singular if and only if these three lines are linearly dependant (all parallel to a single line or all intersecting at a single point). Due to the geometry of the mobile platform, these lines can never be parallel to a single line. Also, if we constrain points O_i to be inside the linear bearings, then the only possibility for these lines to intersect at one point is for the three pivots to coincide with point C, which is impossible under the assumed feasibility conditions.

Therefore, we may state that as long as the pivots are constrained to move inside the linear bearings (or equivalently, as long as point C is constrained to move within the circular path), this mechanism does not have any singularities.

VII. Workspace Analysis

The most advantageous feature of this mechanism is that its local properties over *xy* are identical for any orientation of the mobile platform, but rotated at the orientation angle. Thus, the set of locations that are attainable by point *C* for a given orientation (referred to as *constant-orientation workspace* [7]), under some given feasibility conditions, are needed to be found only for the orientation $\theta = 0$.

In practice, the linear bearings will not reach point *C* (Fig. 4). Let ε be the offset distance from point *C* to the beginning of the feasible range for point O_i. Once again, a geometric method may be used to determine the workspace of this robot. For a constant orientation, the intersection of three regions (see the green hatched region) needs to be computed. This would be the constant-orientation workspace. Then, it is obvious that for another orientation, the workspace would be the same but rotated about *O*.

Now, what is certainly of main interest is the area that is accessible by point *C* for *any* orientation (the so-called *dextrous workspace*). What is great about this robot is that this area is a disk (the one in red).

For brevity, the exact geometric algorithm will not be presented here. This algorithm may be used to optimize the dextrous workspace of this robot and set the optimum length of the feasible range for point O_i (i.e., the length of the linear bearings). It is easy to show that this optimum length is equal to $1-\varepsilon$, in which case the dextrous workspace of this mechanism is a disk of radius $1-\varepsilon$.

Note that this dextrous workspace is easily achievable in practice. Indeed, with a reasonably small value for ε, there would be no other mechanical limits restraining the workspace. Furthermore, the resulting dextrous workspace will have no singularities and, as it will be shown in the next section, the robot will have a fairly high and uniform accuracy inside this circular dextrous workspace.

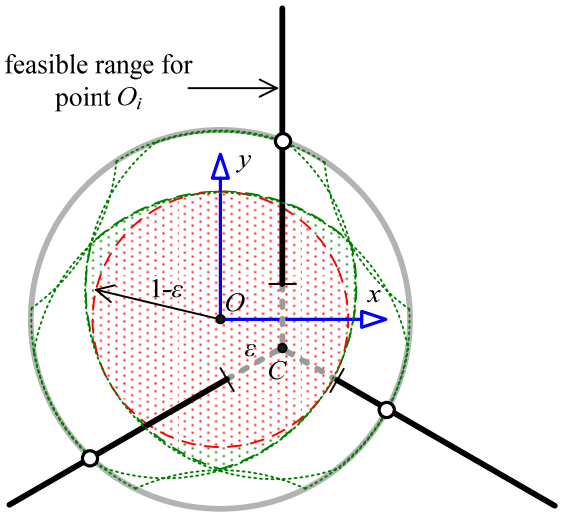

Fig. 4. Dextrous workspace of the parallel robot under study.

VIII. Local Dexterity Analysis

A dexterity analysis can be applied to the system now that the Jacobian matrix is known. Dexterity is defined as the capability of the robot to make accurate movements and is a measure of its kinematic accuracy [5]. To characterize the accuracy of a robot's dexterity, an expression was established using its Jacobian matrix. The Jacobian matrix is used because it is the linear transformation between Cartesian and actuator velocities. The local dexterity is the quality of that transformation. The local dexterity index will be defined as [5]:

$$\xi = \frac{1}{\|\mathbf{J}\|\|\mathbf{J}^{-1}\|}, \tag{18}$$

where

$$\|\mathbf{J}\| = \sqrt{tr\left(\frac{1}{3}\mathbf{J}\mathbf{J}^T\right)}. \tag{19}$$

The local dexterity is limited between 0 and 1—the higher its value, the more accurate the robot. When the local dexterity is equal to 1, it is said that the robot is isotropic at the given pose. Inversely, when the local dexterity is equal to zero, it is said that the robot is at a singular configuration.

As already mentioned, any kinematic performance index for this parallel robot will lead to the same plot over the position workspace, but the plot will be rotated by the orientation angle. Therefore, the local dexterity plot will be shown only for $\theta = 0$.

Figure 5 shows the local dexterity contour plot for the parallel robot under study, over a dextrous workspace of radius 0.8. As can be seen, the closer the center of the mobile platform to the center of the circular path, the higher the local dexterity. The maximum value is nearly 0.95. The local dexterity drops exponentially when nearing the circular path, but, inside the dextrous workspace of radius 0.8, the local dexterity drops only to about 0.79, which is a relatively small decrease. Therefore, the parallel robot has a fairly high and uniform dexterity.

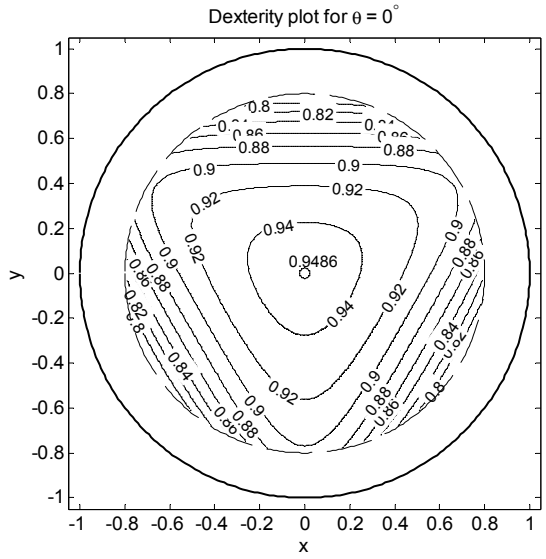

Fig. 5. Local dexterity contour plot for the parallel robot under study.

IX. CONCLUSION

A brief but complete study of the kinematics of an unknown planar parallel robot with circular dextrous workspace was presented in this paper. It was shown that simple elegant solutions exist to all problems involved in the kinematic design and control of this robot. Finally, it became obvious that the parallel robot has a fairly high and uniform kinematic accuracy inside its circular dextrous workspace. Thus, a good mechanical design in which the mobile platform is supported on the three pivots will ensure a very rigid structure that is suitable for precision positioning.

X. REFERENCES

[1] J.-P. Merlet, *Parallel Robots*, 2nd ed., Springer, The Netherlands.

[2] I.A. Bonev and C.M. Gosselin, "Geometric Algorithms for the Computation of the Constant-Orientation Workspace and Singularity Surfaces of a Special 6-RUS Parallel Manipulator," *ASME Design Engineering Technical Conferences*, Montréal, Canada, September 29 – October 2, 2002.

[3] A. Scheidegger and R. Liechti, "Positioning Device," US Patent No. 6,622,586, filed on December 21, 2001, issued on September 23, 2003.

[4] I.A. Bonev, D. Zlatanov, and C.M. Gosselin, "Singularity Analysis of 3-DOF Planar Parallel Mechanisms via Screw Theory," *ASME Journal of Mechanical Design*, Vol. 125, No. 3, pp. 573–581, 2003.

[5] C. Gosselin, "The optimum design of robotic robots using dexterity indices," *Robotics and Autonomous systems*, Vol. 9, pp. 213-226, 1992.

[6] J.-P. Merlet, "Direct Kinematics of Planar Parallel Manipulators," *Proceedings of the 1996 IEEE International Conference on Robotics and Automation*, Minneapolis, Minnesota, April, 1996.

[7] J.-P. Merlet, C.M. Gosselin, and N. Mouly, "Workspaces of Planar Parallel Manipulators," *Mechanism and Machine Theory*, Vol. 33, No. 1/2, pp. 7-20, 1998.